Cancer Chemother Pharmacol (2011) 68:325–335
DOI 10.1007/s00280-010-1486-7

ORIGINAL ARTICLE

The PI-3 kinase-Akt-MDM2-survivin signaling axis in high-risk neuroblastoma: a target for PI-3 kinase inhibitor intervention

Susan K. Peirce · Harry W. Findley · Chengyu Prince · Anindya Dasgupta · Todd Cooper · Donald L. Durden

Received: 29 October 2009 / Accepted: 4 October 2010 / Published online: 24 October 2010

Abstract
Purpose Studies of SF1126, an RGDS targeted, water-soluble prodrug of LY294002, are currently nearing completion in two adult Phase I trials. Herein, we performed a preclinical evaluation of SF1126 as a PI-3K inhibitor for Phase I trials in the treatment of recurrent neuroblastoma (NB).
Methods The effects of SF1126 on pAkt-MDM2 cell signaling, proliferation, apoptosis, and migration were determined using a panel of NB cell lines, and anti-tumor activity was determined using a xenograft model of NB.
Results SF1126 blocks MDM2 activation, IGF-1 induced activation of Akt, and the upregulation of survivin induced by IGF-1. It also increases sensitivity to doxorubicin in vitro and was found to exhibit marked synergistic activity in combination with doxorubicin. Treatment disrupts the integrin $\alpha v\beta 3/\alpha v\beta 5$-mediated organization of the actin cytoskeleton as well as the $\alpha 4\beta 1/\alpha 5\beta 1$-mediated processes essential to metastasis. In vivo, SF1126 markedly inhibits tumor growth in NB xenografted mice ($P < 0.05$).
Conclusions A pan PI-3 kinase inhibitor has potent anti-tumor activity and induces apoptosis in multiple neuroblastoma cell lines. The observed effects of SF1126 on the p-Akt-MDM2-survivin axis suggest a patient selection paradigm in which NB tumors with increased pAkt-MDM2-survivin signaling may predict response to SF1126 alone or in combination with standard chemotherapy regimens that contain anthracyclines.

Keywords Pan PI3-kinase inhibitor · SF1126 · Neuroblastoma · MDM2 · Survivin

Introduction

Neuroblastoma (NB) is the most common extracranial solid tumor diagnosed in children and high-risk disease carries a dismal prognosis even with aggressive therapy [1, 2]. Nearly half of patients diagnosed with this disease have high risk metastatic disease at the time of presentation. As a result, the prognosis for patients with high risk NB is extremely poor even with aggressive chemotherapy, radiotherapy, and bone marrow transplantation [3, 4].

The PI-3 kinase-Akt pathway is a key convergent pathway, and PI-3 kinase is a critical signaling hub downstream of multiple growth factor receptors including TrkB, VEGFR, PDGFR and EGFR [5–7]. It has been shown to mediate important proliferation and survival signals, both in tumor and endothelial cells. Activation of Akt via growth factor receptor signaling is seen in numerous malignant tumor cell lines and in cancer progression [8]. The IGF system has been shown to be important in the proliferation of

Electronic supplementary material The online version of this article (doi:10.1007/s00280-010-1486-7) contains supplementary material, which is available to authorized users.

S. K. Peirce · H. W. Findley · C. Prince · A. Dasgupta · T. Cooper · D. L. Durden
Department of Pediatrics,
Division of Hematology and Oncology,
Emory University School of Medicine,
Aflac Cancer Center and Blood Service,
Children's Healthcare of Atlanta,
2015 Uppergate Drive, Atlanta, GA 30322, USA

D. L. Durden (✉)
Department of Pediatrics,
Division of Hematology and Oncology, Rady Children's Hospital,
Moores UCSD Cancer Center, University of California,
San Diego, La Jolla, CA 92093-0820, USA
e-mail: ddurden@ucsd.edu

neuroblastoma and exerts its effects through the Type 1 IGF receptor (IGF-1R) [9–13]. Very recent research has focused on targeting IGF-1R in neuroblastoma using a humanized monoclonal antibody to block interaction with its ligand, IGF-1 [13].

Increased expression of either MDM2 or survivin has been linked to poor prognosis in a variety of tumors, but the clinical significance of elevated co-expression of these anti-apoptotic factors has not been reported. In neuroblastoma, increased MDM2 expression due to gene amplification has been demonstrated in several cell lines established from tumors at relapse, and elevated MDM2 has been linked to chemoresistance and inactivation of the p53 pathway [12]. Similarly, elevated expression of survivin in primary neuroblastoma tumors has been associated with increased risk of relapse [14, 15].

Studies of the PI-3 kinase-Akt-mTOR pathway and its effect on the development of malignancies have led to the use of inhibitors to alter the pathophysiology of these malignancies, including NB. Insulin receptor substrate 1 (IRS1) normally plays a key role in transmitting signals from IGF-1 receptors to the PI-3K/Akt pathway. In contrast, mTOR inhibition upregulates IGF-1R signaling through stabilization of IRS1, leading to the paradoxical activation of the PI-3K/Akt/mTOR pathway in NB cancer cell lines and in NB patients treated with mTOR inhibitors, such as rapamycin, temsirolimus and RAD001 [16, 17]. Importantly, mTOR inhibitors have also been shown to activate Akt via the TORC2-dependent phosphorylation of S473 site of Akt and PI-3 kinase inhibitors are known to block the positive feedback activation of Akt [18]. This information has driven research efforts to develop treatment strategies involving rational combinations of agents or single agents that target multiple pathways in pediatric cancers, and underscores the need for a central targeting agent, such as a pan-PI3-kinase inhibitor for treatment of pediatric tumors such as NB.

One such compound, LY294002 (SF1101), has antitumor and antiangiogenic activities in vivo [19]. This small molecule also has inhibitory activity against all isoforms of PI-3 kinase, mTOR, PLK, and PIM1 kinases (Garlich, personal communication and AACR poster, 2010). However, the chemical, pharmacological, and toxicological data for LY294002 prevent it from being a viable drug candidate. Recently, SF1126, a water-soluble, clinically viable, tumor-targeted prodrug form of LY294002 was developed by Semafore Pharmaceuticals; it is currently completing two Phase I adult trials [20]. The chemical design of SF1126 combines an integrin-targeted (primarily $\alpha v\beta 3$ and $\alpha 5\beta 1$) RGDS peptide linked to LY294002 which inhibits all classes of PI-3K (Fig. 1). We have previously described the preclinical evaluation of PK, PD, and antitumor/antiangiogenic activity of SF1126 [21] and we have reported that

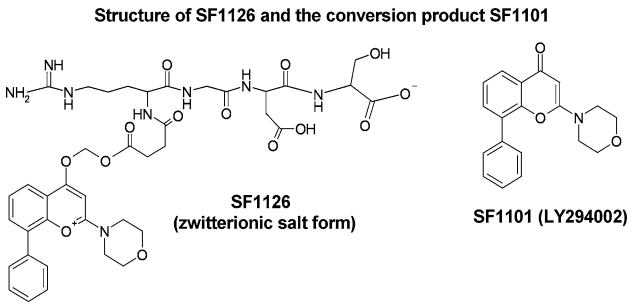

Fig. 1 Structures of SF1101/LY294002 and SF1126. SF1126 combines an integrin-targeted ($\alpha v\beta 3/\alpha 5\beta 1$) RGDS peptide with SF1101/LY294002, which inhibits all members of the PI-3 kinase family. SF1126 remains stable at acidic pH (pH < 5) and spontaneously hydrolyzes at physiologic pH (pH 7)

high risk NB tumors express high levels of $\alpha v\beta 3$ and $\alpha v\beta 5$ integrins in the stromal/endothelial compartment [22]. Hence, SF1126 was designed to target the large number of tumors expressing RGD-binding $\alpha v\beta 3$ integrins including high risk NB. In a very recent paper, we also report that SF1126 is able to reverse trastuzumab resistance in breast cancer cells [23].

Our current data support a clinical trial of SF1126 in recurrent/relapse neuroblastoma. We provide evidence that SF1126 inhibits the phosphorylation of Akt and MDM2 in NB cells and that this inhibition is dependent upon RGDS binding to NB cells in vitro. We found that SF1126 confers significantly increased sensitivity to doxorubicin in NB cell models, supporting its use as a combination agent. We also found that SF1126 treatment inhibits actin-directed cytoskeleton reorganization and cell migration, critical to angiogenesis and metastasis. Thus, in this work, we demonstrate that SF1126 effectively targets the PI-3K/Akt/MDM2 axis in NB cells. Because elevated pAkt and MDM2 expression are often seen at relapse in NB and are associated with chemoresistance, the preclinical studies presented here provide important information about SF1126 as we move toward clinical application of this novel agent to treat NB.

Materials and methods

Cell lines and reagents

NB cell lines (SK-N-BE(2), SH-SY5Y, SK-N-MC, SH-EP1, SK-N-AS, SK-N-F1, LA1-5S, SK-N-SH) were purchased from the American Tissue Culture Collection (Rockville, MD). Cell lines NB-1691, NB-EB, NB-1643, and NB-SD were obtained directly from Sloan Kettering, St. Jude's CRH, CHLA or Children's Memorial Hospital, respectively. SK-N-F1 (a Sloan Kettering line) was obtained from B. Spengler at Fordham University. SK-N-BE(1) cells were provided by C.P. Reynolds (USC-CHLA) (See Supplementary

Data C for full description of cell lines). All cells were maintained in RPMI + 10% FBS. NB-SD, NB-1643, NB-1691, SK-N-BE(1), and SH-SY5Y cells contain wild-type p53; SK-N-BE(2) and NB-EB cells contain p53 mutations. SF1126 for these studies was supplied by Semafore Pharmaceuticals, Inc. (Indianapolis). Antibodies specific for Akt, phospho-S473-Akt, p53, MDM2, phospho-S166-MDM2 and PARP were obtained from Cell Signaling Technology (Danvers, MA) and were used at the manufacturer's recommended concentrations. Vitronectin and fibronectin were purchased from BD Biosciences (Boston). All other reagents were purchased from Sigma (St. Louis) unless otherwise stated.

Proliferation assays

Cells were added to a 96-well plate at a concentration of 2–5 $\times$ 10^4/100 µl per well 24 h before treatment, unless otherwise noted. Following 24–48 h treatments and vehicle alone controls, a water-soluble tetrazolium dye solution (WST-1: Roche; Germany) was added to each well and allowed to incubate at 37°C for 1–2 h. Absorbance was recorded at 450 nm with a test reference of 620 nm using a standard 96-well plate reader, and calculations were made after subtracting the OD of medium alone. For log-transformed SF1126 concentration, nonlinear regression curve fit and determination of IC_{50}, Graph Pad Prism software was used (Graph Pad Software, Inc., La Jolla, CA). For combined dose effect analysis and analysis of synergism, two methods were used. The first, the isobologram method, defined the doses of doxorubicin and SF1126 used to produce a single-agent effect, the $IC_{50,}$ and these doses were plotted on the *x* and *y* axes. The line connecting these two points is the line of additivity, and the response of the two drugs used in combination at their IC_{50} levels were added to this plot. This combined effect is defined as synergistic, additive, or antagonistic when the point lies below, on, or above the line of additivity, respectively. The second method, the combination index (CI), employed a constant ratio two drug combination, diagonal design using CalcuSyn software to apply the Chou–Talalay equation (Biosoft, Ferguson, MO). Both methods are reviewed fully in reference [24].

Biochemical analyses

Cell lysates were analyzed by WB as previously described [20]. To evaluate the effects on Akt and MDM2 phosphorylation, NB cells were treated with 1, 5, 10, or 20 µM SF1126 for 60 min at 4 concentrations, or at a single concentration over a 1 h time course. To detect apoptosis, we examined levels of PARP and cleaved PARP following 4–24 h SF1126 treatment at 5 and 20 µM. For analysis of stimulation by IGF-1, serum-starved cells were treated for 1 and 24 h at 5 and 10 µM concentrations of SF1126, in combination with 100 ng/ml IGF-1 (Sigma, St. Louis, MO). To examine the binding specificity of SF1126 to its RGDS targets, cells were pretreated with 50 µM RGD for 0.5 h.

Actin dynamics and transwell migration assays

NB cells (SK-N-BE(2)) were seeded onto vitronectin-coated cover slips in six well plates. Cells were treated with 25 µM SF1126 for 30 min. Cortical polymerized actin structures were visualized by Phalloidin 555 staining, and nuclei were stained with DAPI. Stained cells were photomicrographed for actin polymerization using confocal microscopy, and cells were imaged using a Zeiss (Thornwood, NY) LSM 510 Meta confocal microscope with a 63× (1.4-numerical-aperture) or 100× (1.4-numerical-aperture) Plan-Apochromat oil objective. All images were acquired using Zeiss LSM 510 software and processed using Adobe Photoshop 7.0 as described elsewhere [25]. To assess cell migration, the bottom surfaces of transwell migration chambers (8 µM Transwell Permeable Supports, Corning) were coated with 20 µg/ml of fibronectin for 2 h at 37°C. SKNBE(2) cells were treated with 0, 5, or 20 µM SF1126 for 0.5 h, washed, trypsinized, and added to the top chambers (2.0 $\times$ 10^5 cells in 200 µL serum-free RPMI); the lower chambers were filled with 600 µL serum-free RPMI. Following a 4-h incubation at 37°C, migrating cells were fixed and stained with a crystal violet solution. Nine 1 mm^2 fields were counted for each treatment, and cells were photographed at 200× with an Olympus PX50. A Student's *t* test was used to determine levels of significance.

Tumor xenograft studies

Athymic female mice (CD-1 *nu/nu*, 20–25 g) were used for in vivo tumor growth inhibition studies. Mice were obtained from the NIH/NCI repository and housed on a 12-h light/dark cycle with food and water ad libitum under pathogen-free conditions, according to the guidelines of the AAALACI. Tumors derived from NB cell lines were generated by harvesting cells from mid-log phase cultures. Five million SKNBE(2) cells in 100 µl PBS were injected subcutaneously (s.c.) into the right flank of each mouse. Tumor growth was monitored twice per week for external measurements using Vernier calipers. Tumor volume was calculated using the formula $V = (A \times B^2)/2$ where *A* and *B* represent length and width of the tumor respectively. Treatment for the antitumor efficacy studies was initiated when tumors in all mice ranged in size from 80 to 100 mm^3. Mice were divided randomly into two groups receiving vehicle (acidified sterile water diluents for SF1126) or SF1126. All treatment was administered *s.c* on the left flank

for 18 days at a dose of 50 mg/kg and at a frequency of 3 times weekly. The route of SF1126 administration and the site of s.c. injection were chosen to most closely mimic slow IV infusion in human Phase I trials and to avoid localized concentrations near the tumor site. No toxicities were noted in mice treated with SF1126 or vehicle. The Student's *t* test was used to compare tumor volume differences between SF1126 treatments and vehicle-treated controls.

Results

SF1126 inhibits proliferation, induces apoptosis, enhances the sensitivity to doxorubicin, and reduces levels of pAKT and pMDM2 in NB cell lines

To assess the ability of SF1126 to inhibit cell viability**,** we evaluated the effects of SF1126 singly and in combination with doxorubicin on NB cell survival. We determined single-agent IC_{50}s for twelve NB cell lines (Fig. 2a; Supplementary Data A) and found that the NB-EB cell line was the most sensitive (IC_{50} 0.95 μM) and NB-SD the least sensitive (IC_{50} 65.7 μM).

When used in combination with chemotherapy, SF1126 significantly increased sensitivity to pharmacologically relevant concentrations of doxorubicin (0.02–1.0 μM) (Fig. 2b, top panel)**,** in all three cell lines examined. By isobologram analysis, two cell lines (SK-N-BE(1) and SK-N-BE(2)) responded synergistically to the combined IC_{50} treatment (Fig. 2b, bottom panel), while the SH-SY5Y cell line responded in an additive manner at this dose level. We performed analyses of synergy with fixed-ratio dose–response curves, using the Chou and Talalay combination index (CI) method [24]. Using this method, the value of a CI indicating a very strong synergism is <0.1, while a range of 0.1–0.3 indicates a strong synergism. Our results indicate a very strong to strong synergy with CI values of 0.17544, 0.11927, and 0.08385 for combined IC_{50s}, IC_{70s}, and IC_{90s}, respectively, for the SK-N-BE(1) cell line. To ascertain the role of apoptosis, we examined the effects of SF1126 treatment on the cleavage product of the DNA repair enzyme PARP. Following a 4- and 24-h treatment of SH-N-SH and SK-N-BE(1) cells with SF1126 (Fig. 2c), we observed a marked increase in the cleaved form of the PARP protein (89 kD) at 24 h at both concentrations of SF1126, indicating that SF1126 induces DNA instability and caspase 3 induction in its promotion of apoptosis.

We next surveyed the phosphorylation status of Akt and/or MDM2 following SF1126 treatment using immunoblotting in NB cell lines SH-SY5Y, SK-N-BE(1), NB-1691, and NB-EB and found that pAkt and constitutively elevated pMDM2 were both reduced in a dose and time-course-dependent manner, indicating that SF1126 blocked activation of both Akt and its substrate MDM2. The MDM2 protein can occur in multiple forms as a result of alternative splicing; however, the roles of these alternate spliced isoforms are not fully understood. In the current study, both the larger (90 kD) and a smaller isoform are evident as both unphosphorylated and phosphorylated proteins in SH-SY5Y and NB-1691 NB cells (Fig. 2d). Notably, the full-length phosphorylated MDM2 protein decreases with increasing SF1126 dosage in SH-SY5Y cells, whereas the shorter phosphorylated isoform decreases in the NB-1691 cells.

SF1126 inhibits survivin expression, MDM2 activation, and IGF-1-induced Akt phosphorylation in an RGDS-dependent manner

Members of the insulin-like growth factor (IGF) family are important proliferative factors for NB and act through the Akt pathway; recent evidence has shown that IGF-1 is involved in conferring resistance to doxorubicin [11]. We investigated the ability of SF1126 to inhibit IGF-1-driven Akt phosphorylation in two NB cell lines, SH-SY5Y and SK-N-BE(1) (Fig. 3a, top panel). Cells were treated with IGF-1/SF1126 for 1 h and over a 24-h period; both treatments reversed IGF-1-mediated Akt phosphorylation.

IGF-1 receptor stimulation activates Akt, upstream of the survival signaling of MDM2 and survivin [11, 17]. We therefore investigated IGF-driven survivin upregulation and the inhibition of this upregulation by SF1126. SF1126 at both 5 and 20 μM effectively inhibited this upregulation (Fig. 3a, bottom panel). To demonstrate the binding specificity of SF1126, we pretreated cells with the RGDS peptide alone and reversed the SF1126-induced inhibition of Akt activation (Fig. 3b, top panel), confirming that the targeted activity of SF1126 is dependent on the RGD moiety and its specific binding to cells.

MDM2 expression and activation are initially upregulated in response to genotoxic stress. MDM2, in turn, targets p53 for ubiquitination and degradation. Thus, this negative feedback loop inhibits p53 function following genotoxic stress [26, 27]. The translocation of MDM2 into the nucleus requires phosphorylation by Akt near the nuclear translocation signal at S166/186 [5]. We investigated the ability of SF1126 to inhibit this negative regulation and found that it blocked the phosphorylation of MDM2 induced by genotoxic stress, thus inhibiting its ability to downregulate p53 (Fig. 3b, bottom panel).

SF1126 disrupts the actin cytoskeleton

Many studies have shown a major role for the small GTPase, Rac1, in the regulation of actin polymerization and hence, integrin-directed migration [28–30]. The ability

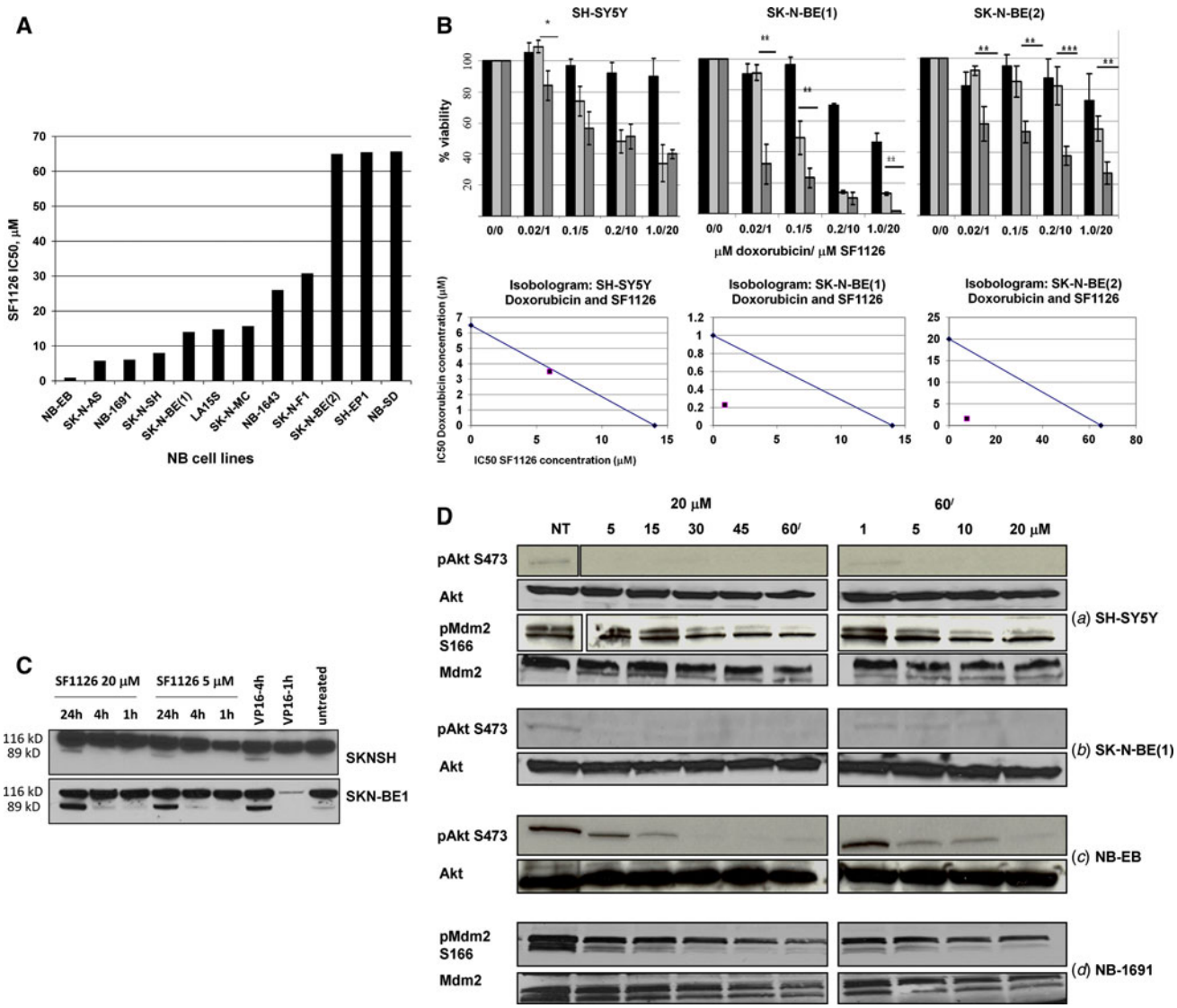

Fig. 2 SF1126 sensitizes neuroblastoma cell lines to doxorubicin treatment, induces PARP cleavage, and blocks Akt and MDM2 activation. **a** IC_{50}s for *twelve NB cell lines*, taken from log transformed SF1126 concentrations and nonlinear regression curve fit (Supplementary Data A). **b** *Top panel* quantification of cell proliferation using the tetrazolium-based colorimetric assay, WST-1, following 24 h SF1126 and/or doxorubicin treatments. Results are compiled from 3 to 5 separate experiments and means ± SD are shown. *Black box* SF1126 alone. *Grey box* doxorubicin alone. *Dark grey box* 20 μM SF1126 + doxorubicin. $*P < 0.05$, $**P < 0.01$, $***P < 0.005$. **b** *Bottom panel* isobologram analysis of combined IC_{50} doses of doxorubicin and SF1126. Line connecting single IC_{50} doses is the line of additivity, and the response of the two drugs used in combination at their IC_{50} levels are indicated on these *plots*. The combined effect is defined as synergistic, additive, or antagonistic when the point lies below, on, or above the line of additivity, respectively. **c** SF1126 treatment of SK-N-SH and SN-N-BE(1) cells increased levels of the PARP cleavage product. Cells were treated for 1, 4, and 24 h at 5 and 20 μM. 116 kD = full length PARP; 89 kD = cleaved PARP. **d** Analysis of Akt and MDM2 inactivation following SF1126 treatment in NB cell lines. Subconfluent neuroblastoma cell lines (*a*) SH-SY5Y, (*b*) SK-N-BE(1), (*c*) NB-EB, and (*d*) NB-1691 were incubated with 20 μM SF1126 for 5, 15, 30 45 or 60 min (*left*) or at 1, 5, 10 or, 20 μM concentrations for 60 min (*right*). *NT* no treatment

to block the migratory and invasive capacity of tumor cells offers an important avenue for treating patients with malignant disease, and unpublished observations from our laboratory as well as reports by other laboratories indicate that PI-3 kinase activity is required for Rac1-induced cell motility [31–33]. Herein, we demonstrate marked disruption of actin cytoskeletal filaments following SF1126 treatment, in NB cells attached to vitronectin (Fig. 4a). Untreated cells display features consistent with polarization and movement, including strong F-actin staining in the extended lamellipodia and filopedia (arrows). In contrast, the SF1126-treated cells are contracted with disorganized actin

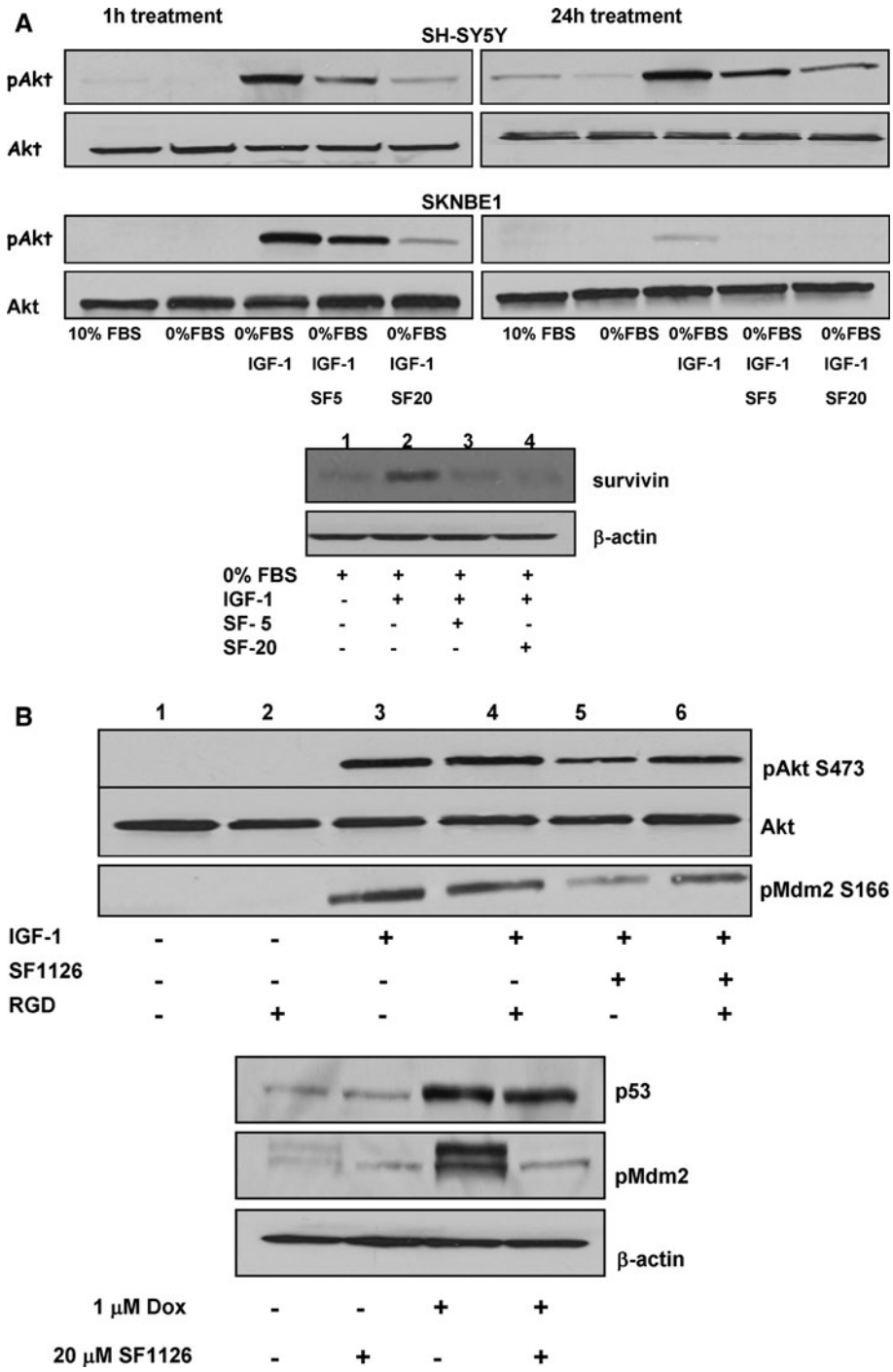

Fig. 3 SF1126 inhibits Akt-driven signaling pathways, survivin expression, and p53-MDM2 feedback via RGDS-binding specificity. **a** *Top panel* SF1126 treatment (5 and 20 μM) inhibits the IGF-1-induced activation of Akt in SH-SY5Y and SK-N-BE(1) NB cell lines. Cells were either left untreated in 10% FBS or serum starved (0% FBS). To treat cells in the presence or absence of 5 or 20 μM SF1126, 100 ng/ml of IGF-1 was used. Cells were treated for 1 h (*left*) or for 24 h (*right*). **a** *Bottom panel* SF1126 inhibits survivin upregulation via the PI3K/Akt pathway. Serum-starved SK-N-BE(1) cells were treated with 100 ng/ml IGF-1 in the presence or absence of SF1126 (5 and 20 μM). **b** *Top panel* RGD pretreatment blocks SF1126 inhibition. SH-SY5Y cells were pulsed with 50 μM RGD for 0.5 h, washed, then stimulated with 100 ng/ml IGF-1 in the presence or absence of 5 μM SF1126 for an additional 24 h. **b** *Bottom panel* SF1126 inhibits the p53-MDM2 feedback loop. Doxorubicin (0.1 μM) both upregulates p53 and induces the activation of Mdm2; SF1126 inhibits this activation. SHSY5Y cells were treated with 0.1 μM doxorubicin and/or SF1126 (20 μM) for 4 h

structures, and lack polarized orientations. From these data, we can conclude that SF1126 inhibits PI3-K activity required by the actin cytoskeletal integrity.

SF1126 inhibits fibronectin-induced migration

Neuroblastoma is a highly metastatic tumor, a primary cause of death in NB patients [1], and integrin-mediated migration is a necessary step for invasion and metastasis. Based on our findings that SF1126 disrupts the organization of the actin cytoskeleton, we investigated the effects of SF1126 on cell migration. Fibronectin is the major extracellular matrix protein, and it binds to the integrin receptors, $\alpha 5\beta 1$ and $\alpha 4\beta 1$. The mean number of migrating cells in the fibronectin alone control group was 222/mm^2 ($\pm$22), while the mean number of cells migrating on fibronectin with 5 and 20 μM SF1126, respectively, was 81 ($\pm$13) and 52 ($\pm$9) cells/mm^2 ($P < 0.01$) (Fig. 4b). Thus, SF1126

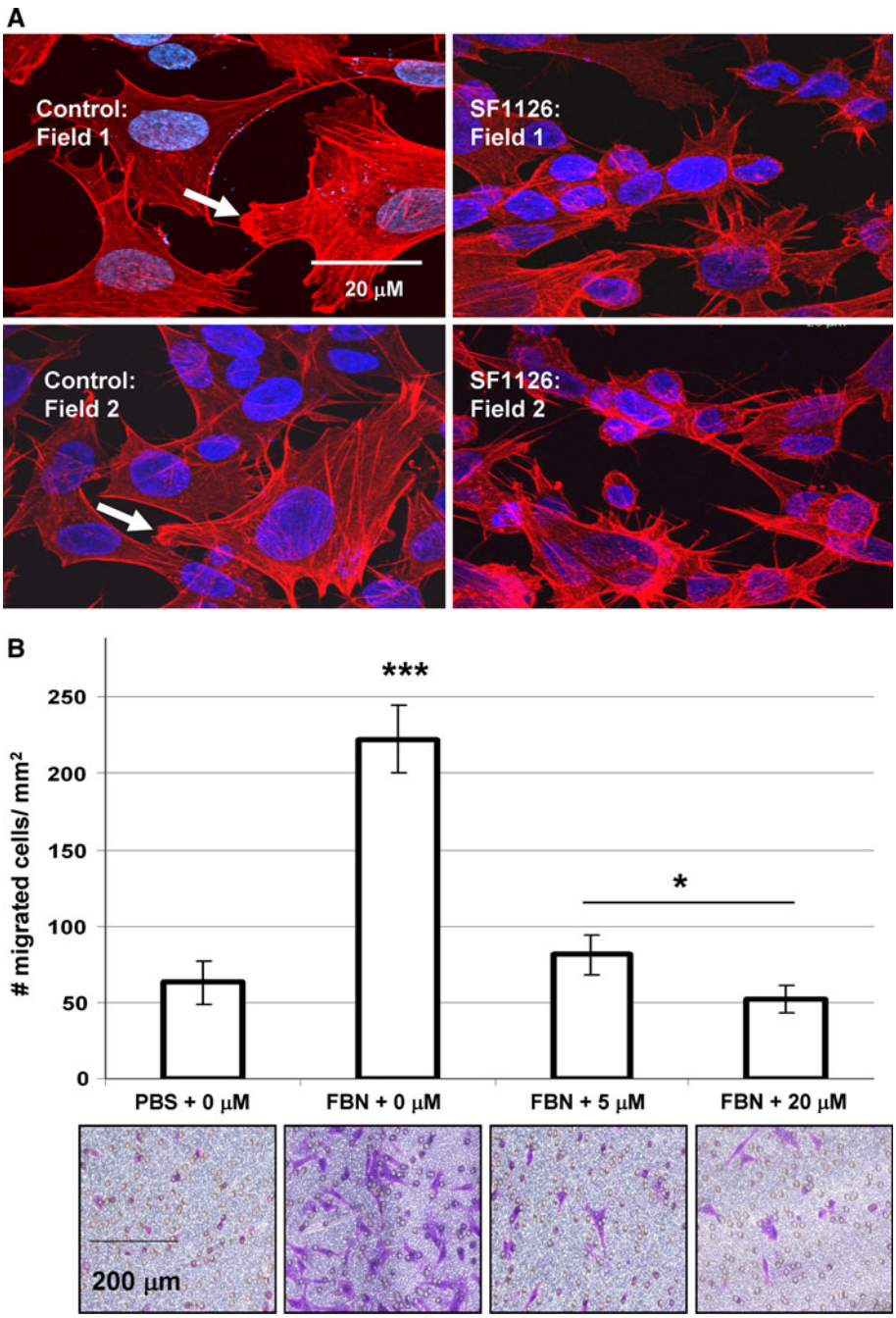

Fig. 4 SF1126 blocks actin polymerization and alters cytoskeletal organization and cell migration. **a** Effect of SF1126 on the state of actin polymerization in NB cells. SK-N-BE(2) cells were plated on vitronectin and treated with SF1126 (25 μM) for 30 min. Fixed cells were processed for confocal microscopy (see details in "Materials and methods"). Two different fields are shown, with and without SF1126 treatment. **b** SF1126 treatment inhibits matrix protein (fibronectin)-induced cell migration. SK-N-BE(2) cells were treated with 5 or 20 μM SF1126 for 30 min (see details in "Materials and methods"). $^{*}P < 0.05$, $^{***}P < 0.005$. *FBN* fibronectin

inhibits $\alpha4\beta1/\alpha5\beta1$-mediated migration, a process essential to metastasis.

Antitumor activity of SF1126 in a NB xenograft model

With the knowledge of the inhibitory effects of SF1126 on SK-N-BE(2) cell proliferation, actin organization, and migration, we next tested the antitumor efficacy of SF1126 in a SKNBE(2) tumor xenograft model (Fig. 5). SF1126 demonstrated robust antitumor activity, and growth rates of tumors were significantly different from vehicle-treated mice ($n = 7$, $P < 0.05$). The mean tumor volumes between the control and the SF1126 groups differed significantly starting at 4 days following treatment (802 ± 466 mm^3 vs. 173 ± 37 mm^3, respectively), and these differences continued through the last day of treatment ($2{,}277 \pm 932$ mm^3 vs. 579 ± 65 mm^3). SF1126-treated mice showed no evidence of toxicity, as measured by body weight and survival relative to control animals.

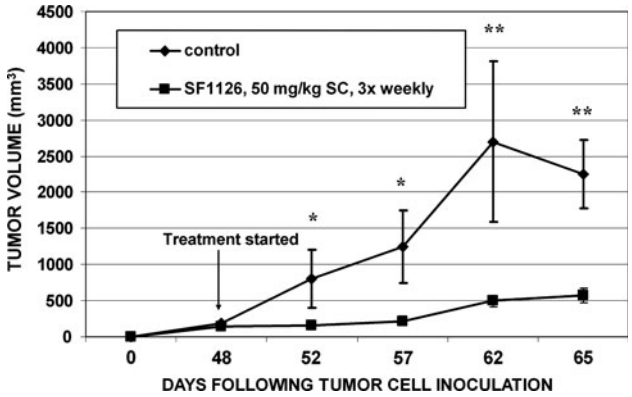

Fig. 5 SF1126 inhibits tumor growth in a xenograft model: effect of SF1126 treatment in a human xenograft model. SK-N-BE(2) cells were implanted *sc* in the left flank of athymic mice as described in "Materials and methods". Animals were treated with 50 mg/kg SF1126 on QOD 3 times a week by subcutaneous injection starting on day when average tumor volume was 90–100 mm^3. Tumor volumes were measured twice a week. Difference in tumor volumes at days 4 and 9 after the start of therapy between control vehicle-treated mice and SF1126-treated animals were statistically significant at $*P < 0.05$. The differences on days 14 and 17 were determined to be highly significant at $**P < 0.01$. This experiment is representative of three experiments performed

Discussion

There is a significant need for the development of novel effective therapies for the treatment of NB. In the current study, we describe the preclinical efficacy of an RGDS-conjugated pan-PI-3 kinase inhibitor, SF1126, in the inhibition of NB tumor growth in vivo and the chemosensitization of NB tumor cells to doxorubicin exposure in vitro. We have defined a signaling pathway in primary tumors and NB cell lines which may predict responsiveness to pan PI-3 kinase inhibition and lead to patient selection efforts in future Phase I trials. Unfavorable NBs usually express TrkB, a tyrosine kinase receptor, and its ligand brain-derived neurotrophic factor (BDNF). Our rationale for application of pan PI-3 kinase inhibitors to NB therapeutics is based on studies of the role of known receptor-ligand interactions in stimulating NB growth and chemoresistance, including but not limited to TrkB and its ligand BDGF [2, 34, 35, 38–40] and IGF-1 [36, 37]. BDNF has been shown to protect cells from chemotherapy, and it is known that the phosphorylation of Akt is central to BDNF activation of TrkB signaling [35, 38, 41].

Thus, it has become increasingly apparent that the most effective targeted therapeutic agents are inhibitors that block multiple kinases or an intercept point through which multiple cell surface receptor or tyrosine kinases expert downstream signaling effects [42, 43]. Blocking a single function by a specific receptor may fail to prevent other receptors from providing the tumor cells with proliferative/survival, migratory, invasive, or angiogenic signals. Restricted spectrum inhibitors may therefore have limited antitumor activity, and resistance will develop rapidly in vivo. Further, the most successful tyrosine kinase inhibitor, imatinib, exerts its antitumor activity against multiple targets, including BCR/ABL, c-KIT, and PDGFR. FDA approvals of two antiangiogenic agents: sorafenib (Nexavar), in December 2005, and sunitinib (Sutent), in January 2006, represent major landmarks for solid tumor oncology. Sorafenib is an orally administered multi-kinase inhibitor which targets RAF kinase along with VEGFR, PDGFR, c-KIT, and other kinases [44]. This success of multi-kinase inhibitors further supports our efforts to target a point in mammalian signaling through which many cell surface receptors and kinases converge, PI-3 kinase.

Malignant embryonal tumors of childhood, such as NB, are composed of highly motile cells and undergo dramatic alterations in their actin-cytoskeletal organization that facilitate their invasive and migratory behavior. Migration is a process of actin reorganization and is directed by the Rho family of small GTPases, primarily Rac1, Cdc42, and RhoA. Polarized cells extend the membrane structures lamellipodia and filopodia to become the leading cell edge, a process requiring Rac1 and Cdc42, respectively. RhoA, in turn, directs focal adhesion assembly, and cells form new focal adhesions by the creation of actin stress fibers in the extracellular matrix [29–32], allowing them to move forward. In neuronal cell migration, Rac1 and an additional factor, Filamen A, are required cooperatively to induce neurite outgrowth, and the antagonism of Cdc42 and Rac1 is known to inhibit this process [50]. Our data demonstrate that SF1126 markedly deregulates actin filament formation and induces a depolarized and disorganized cytoskeletal actin structure. The morphological changes ultimately resulting in migration require actin polymerization of the lamellipodia, and SF1126 treatment targets this polymerization. Other laboratories have also found that blocking PI-3 kinase activation using pharmacological inhibitors effectively blocks actin polymerization [29, 45], and studies with such inhibitors have established that PI3K/Rac1 and Cdc42 are required for migrating neurons [46–49]. More lines of evidence demonstrate that several specific Rac-regulated cellular functions including assembly of focal complexes and invasiveness require PI-3 kinase activity [29–31]. The activation of Rac1 is dependent on the availability of the guanine exchange factors Vav1 and Vav2. These, in turn, require the PI-3K products PIP_2 and PIP_3 for binding to Rac1 [50]. In this current study, inhibition of PI-3K by SF1126 treatment likely blocked the production of PIP_2 and PIP_3, and ultimately, the conversion of inactive Rac1-GDP to active Rac1-GTP.

Previous reports from our laboratory established that SF1126 blocks tumor progression in vivo using multiple adult tumor xenograft models and demonstrated that SF1126 has both potent antiangiogenic activity and antitumor activity [21]. The current Phase I clinical trial of SF1126 in adults is at dose level 5 or 1,110 mg/m^2/dose (40 mg/kg/dose) and shows minimal toxicity. It is important to note that the in vitro activity of SF1126 in half of the NB cell lines surveyed is well below the highest levels achieved in Phase I clinical trials. Moreover, pharmacokinetics demonstrates levels of SF1126 of 20–30 μM in plasma with evidence of pharmacodynamic inhibition of tumor-associated pAkt in patients treated with SF1126 at this dose [20]. In this current preclinical study, SF1126 demonstrates single-agent antitumor activity in a xenograft model using SK-N-BE(2) NB cells. Since treatment with SF1126 (50 mg/kg on alternate days for 3 weeks) is well tolerated, it is likely that increasing the duration of therapy or dose would have produced tumor regression.

Our results with SK-N-BE(2) cells which are derived from a relapsed resistant p53 mutated tumor suggest that the inhibitory effects of SF1126 on tumor cell survival and tumor growth may be mediated through p53-independent means. Moreover, the use of this relapse NB cell line supports the potential efficacy of SF1126 in the relapsed clinical setting where p53 may be disabled. In addition to p53, a number of other pro-apoptotic proteins are known to bind to the N terminus of MDM2 and are regulated by levels of MDM2 activation; these include E2F1 and p73 [51, 52]. NB relapse patients often develop p53 mutations, conferring much greater resistance to standard chemotherapeutics [12]. Here, we demonstrate that SF1126 efficacy does not require functional p53.

Recent work has shown that the PI-3 kinase-Akt pathway is more significantly altered in high-grade NB tumors and tumors with poor prognostic features [7, 11]. In a limited panel of primary neuroblastoma tumor samples ($n = 18$), we have utilized RT–PCR to generate data which shows a direct correlation between high level coexpression of both survivin and MDM2 mRNA and prognosis as defined by 3 year event free survival rates (Supplementary Data B1, B2, B3). The combined results from our studies suggest that the analysis of pAkt, MDM2, and survivin may serve as surrogate biomarkers to select patients for PI-3 kinase therapeutics. These findings also support the hypothesis that agents that can downregulate both survivin expression and MDM2 activation may provide novel approaches to the treatment of neuroblastoma in the future. The analysis of an expanded cohort of NB patient tumor samples will be required to confirm these observations.

Finally, these results indicate that SF1126 affects NB tumor growth by blocking tumor cell survival, proliferation, and migration required for metastasis. SF1126 generates its effects via multiple signaling pathways in NB cells and through inhibitory effects on NB cell motility and migration. These findings support the evaluation of SF1126 as a single agent or in combination with anthracyclines in neuroblastoma in a pediatric Phase I trial, and tumors with a highly activated PI-3 kinase-Akt-MDM2 pathway may be most responsive to this therapy.

Acknowledgments We thank C. P. Reynolds for his kind gift of NB cells. We would like to thank N. Dey and Adam Marcus for technical assistance with confocal imaging. This work was supported by NIH-CA94233 (DLD), Alex's Lemonade Stand Foundation (DLD), Magic Waters Foundation (DLD) and CURE Childhood Cancer (DLD and HWF).

References

1. Brodeur GM, Neuroblastoma (2003) Biological insights into a clinical enigma. Nat Rev Cancer 3:203–216
2. Ho R, Eggert A, Hishiki T, Mintum JE, Ikegaki N, Foster P, Camoratto AM, Evans AE, Brodeur G (2002) Resistance to chemotherapy mediated by TrkB in neuroblastomas. Cancer Res 62:6462–6466
3. Matthay KK, Villablanca JG, Seeger RC, Stram DO, Harris RE, Ramsay NK, Swift P, Shimada H, Black CT, Brodeur GM, Gerbing RB, Reynolds CP (1999) Treatment of high-risk neuroblastoma with intensive chemotherapy, radiotherapy, autologous bone marrow transplantation, and 13-cis-retinoic acid. N Engl J Med 341:1165–1173
4. Attiyeh EF, London WB, Mosse YP, Wang Q, Winter C, Khazi D, McGrady PW, Seeger RC, Look TA, Shimada H, Brodeur GM, Cohn SL, Matthay KK, Maris JM (2005) Chromosome 1p and 11q deletions and outcome in neuroblastoma. N Engl J Med 353:2243–2253
5. Mayo LD, Donner DB (2001) A phosphatidylinositol 3-kinase/Akt pathway promotes translocation of Mdm2 from the cytoplasm to the nucleus. PNAS-USA 98:11598–11603
6. Takeuchi K, Ito F (2004) Suppression of adriamycin-induced apoptosis by sustained activation of the phosphatidylinositol-3′-OH kinase-Akt pathway. J Biol Chem 279:890–892
7. Boller D, Schramm A, Doepfner KT, Shalaby T, von Bueren AO, Eggert A, Grotzer MA, Arcaro A (2008) Targeting the phosphoinositide 3-kinase isoform p110δ impairs growth and survival in neuroblastoma. Cells Clin Cancer Res 14:1172–1181
8. Osaki M, Oshimura M, Ito H (2004) PI3K-Akt pathway: its functions and alterations in human cancer. Apoptosis 9:667–676
9. Feng Z, Hu W, de Stanchina E (2007) The regulation of AMPK {beta}1, TSC2, and PTEN expression by p53: stress, cell and tissue specificity, and the role of these gene products in modulating the IGF-1-AKT-mTOR pathways. Cancer Res 67:3043–3053
10. Vaira V, Lee CW, Goel HL, Bosari S, Languino LR, Altiero DC (2006) Regulation of survivin expression by IGF-1/mTOR signaling. Oncogene 26:2678–2684
11. Opel D, Poremba C, Simon T, Debatin K-M, Fulda S (2007) Activation of Akt predicts poor outcome in neuroblastoma. Cancer Res 67:735–745
12. Carr J, Bell E, Pearson ADJ, Kees UR, Beris H, Lunec J, Tweedle DA (2006) Increased frequency of aberrations in the p53/MDM2/

p14ARF pathway in neuroblastoma cell lines established at relapse. Cancer Res 66:2138–2145
13. Houghton PJ, Morton CL, Gorlick R, Kolb EA, Keir ST, Reynolds CP, Kang MH, Maris JM, Wu J, Smith MA (2010) Initial testing of a monoclonal antibody (IMC-A12) against IGF-1R by the pediatric preclinical testing program. Pediatr Blood Cancer 54:921–926
14. Islam A, Kageyama H, Takada N, Kawamato T, Takayasu H, Isogai E, Ohira M, Hashizume K, Kobayashi H, Kaneko Y, Nakagawara A (2000) High expression of Survivin, mapped to 17q25, is significantly associated with poor prognostic factors and promotes cell survival in human neuroblastoma. Oncogene 19:617–625
15. Miller MA, Ohashi K, Zhu X, McGrady P, London WB, Hogarty M, Sandler AD (2006) Survivin mRNA levels are associated with biology of disease and patient survival in neuroblastoma: a report from the children's oncology group. J Pediat Hemat Oncol 28:412–417
16. Tao Y, Pinzi V, Bourhis J, Deutsch E (2007) Mechanisms of disease: signaling of the insulin-like growth factor 1 receptor pathway/therapeutic perspectives in cancer. Nat Clin Prac Oncol 4:591–602
17. Shi Y, Yan H, Frost P, Gera J, Lichtenstein A (2005) Mammalian target of rapamycin inhibitors activate the AKT kinase in multiple myeloma cells by up-regulating the insulin-like growth factor receptor/insulin receptor substrate-1/phosphatidylinositol 3-kinase cascade. Mol Cancer Ther 4:1533–1540
18. O'Reilly KE, Rojo F, She Q-B, Solit D, Mills GB, Smith D, Lane H, Hofmann F, Hicklin DJ, Ludwig DL, Baselga J, Rosen N (2006) mTOR inhibition induces upstream receptor tyrosine kinase signaling and activates Akt. Cancer Res 66:1500–1508
19. Vlahos CJ, Matter WF, Hui KY, Brown RF (1994) A specific inhibitor of phosphatidylinositol 3-kinase, 2-(4-morpholinyl)-8-phenyl-4H-1-benzopyran-4-one (LY294002). J Biol Chem 269:5241–5248
20. Chiorean E, Mahadevan D, Harris W, VonHoff DD, Younger AE, Rensvold DM, Shelton CF, Hennessy BT, Garlich JR, Ramanathan RK (2009) Phase 1 evaluation of SF1126, a vascular targeted PI3K inhibitor, administered twice weekly IV in patients with refractory solid tumors. American Society of Clinical Oncology (ASCO), Orlando, FL
21. Garlich JR, De P, Dey N, Su JD, Peng X, Miller A, Murali R, Lu Y, Mills GB, Kundra V, Shu HK, Peng Q, Durden DL (2008) A vascular targeted pan phosphoinositide 3-kinase inhibitor prodrug, SF1126, with antitumor and antiangiogenic activity. Cancer Res 68:206–215
22. Erdreich-Epstein A, Shimada H, Groshen S, Liu M, Metelitsa LS, Kim KS, Stins MF, Seeger RC, Durden DL (2000) Integrins {{alpha}}v{beta}3 and {{alpha}}v{beta}5 are expressed by endothelium of high-risk neuroblastoma and their inhibition is associated with increased endogenous ceramide. Cancer Res 60:712–721
23. Ozbay T, Durden DL, Liu T, O'Regan RM, Nahta R (2009) In vitro evaluation of pan-PI3-kinase inhibitor SF1126 in trastuzumab-sensitive and trastuzumab-resistant HER2-over-expressing breast cancer cells. Cancer Chemther Pharmacol 9:1075–1079
24. Zhao L, Wientjes MG, Au JL-S (2004) Evaluation of combination chemotherapy: integration of nonlinear regression, curve shift, isobologram, and combination index analyses. Clin Can Res 10:7994–8004
25. Dey N, De PK, Wang M, Zhang H, Dobrota EA, Robertson KA, Durden DL (2007) CSK controls retinoic acid receptor (RAR) signaling: a RAR-c-SRC signaling axis is required for neuritogenic differentiation. Mol Cell Biol 27:4179–4197
26. Speidel D, Helmbold H, Deppert W (2005) Dissection of transcriptional and non-transcriptional p53 activities in the response to genotoxic stress. Oncogene 25:940–953
27. Ramalingam S, Honkanen P, Young L, Shimura T, Austin J, Steeg PS, Nishizuka S (2007) Quantitative assessment of the p53-Mdm2 feedback loop using protein lysate microarrays. Cancer Res 67:6247–6252
28. Nakada M, Niska JA, Tran NL, Berens ME (2005) EphB2/R-Ras signaling regulates glioma cell adhesion, growth, and invasion. Am J Pathol 167:565–576
29. Nobes CD, Hall A (1995) Rho, Rac, and Cdc42 GTPases regulate the assembly of multimolecular focal complexes associated with actin stress fibers, lamellipodia, and filopodia. Cell 81:53–62
30. Keely PJ, Westwick JK, Whitehead IP, Der CJ, Parise L (1997) Cdc42 and Rac1 induce integrin-mediated cell motility and invasiveness through PI(3)K. Nature 390:632–636
31. Kapur R, Cooper R, Zhang L, Williams DA (2001) Cross-talk between {alpha}4{beta}1/{alpha}5{beta}1 and c-Kit results in opposing effect on growth and survival of hematopoietic cells via the activation of focal adhesion kinase, mitogen-activated protein kinase, and Akt signaling pathways. Blood 97:1975–1981
32. Hall A (1998) Rho GTPases and the actin cytoskeleton. Science 279:509–514
33. Fruman DA, Meyers RE, Cantley LC (1998) Phosphoinositide kinases. Annu Rev Biochem 67:481–507
34. Hecht M, Schulte JH, Eggert A, Wilting J, Schweigerer L (2005) The neurotrophin receptor TrkB cooperates with c-Met in enhancing neuroblastoma invasiveness. Carcinogenesis 26:2105–2115
35. Middlemas DS, Kihl BK, Zhou J, Zhu X (1999) Brain-derived neurotrophic factor promotes survival and chemoprotection of human neuroblastoma cells. J Biol Chem 274:16451–16460
36. Gil-Ad I, Shtaif B, Luria D, Karp L, Fridman Y, Weizman A (1999) Insulin-like-growth-factor-I (IGF-I) antagonizes apoptosis induced by serum deficiency and doxorubicin in neuronal cell culture. Growth Horm IGF Res 9:458–464
37. Van Golen CM, Feldman EL (2000) Insulin-like growth factor I is the key growth factor in serum that protects neuroblastoma cells from hyperosmotic-induced apoptosis. J Cell Physio 182:24–32
38. Desmet C, Peeper D (2006) The neurotrophic receptor TrkB: a drug target in anti-cancer therapy? Cell Mol Life Sci 63:755–759
39. Edsjo A, Lavenius E, Nilsson H, Hoehner JC, Simonsson P, Culp LA, Martinsson T, Larsson C, Pahlman S (2003) Expression of TrkB in human neuroblastoma in relation to MYCN expression and retinoic acid treatment. Lab Invest 83:813–823
40. Evans A, Kisselbach K, Liu X, Eggert A, Ikegaki N, Camoratto A, Dionne D, Brodeur G (2001) Effect of CEP-751 (KT-6587) on neuroblastoma xenografts expressing TrkB. Med Pediat Oncol 36:181–184
41. Geiger TR, Peeper DS (2005) The neurotrophic receptor TrkB in anoikis resistance and metastasis: a perspective. Cancer Res 65:7033–7036
42. Castellino RC, Durden DL (2007) Mechanisms of disease: the PI3K-Akt-PTEN signaling node/an intercept point for the control of angiogenesis in brain tumors. Nat Clin Pract Neuro 3:682–693
43. Wong S, McLaughlin J, Cheng D, Zhang C, Witte ON (2004) Sole BCR-ABL inhibition is insufficient to eliminate all myeloproliferative disorder cell populations. PNAS-USA 101:17456–17461
44. Kurosa T, Ohki M, Wu N (2009) Sorafenib induces apoptosis specifically in cells expressing BCR/ABL by inhibiting its kinase activity to activate the intrinsic mitochondrial pathway. Cancer Res 69:3927–3936
45. Su JD, Mayo LD, Donner DB, Durden DL (2003) PTEN and phosphatidylinositol 3′-kinase inhibitors up-regulate p53 and block tumor-induced angiogenesis: evidence for an effect on the tumor and endothelial compartment. Cancer Res 63:3585–3592
46. Price LS, Leng J, Schwartz MA, Bokoch GM (1998) Activation of Rac and Cdc42 by integrins mediates cell spreading. Mol Biol Cell 9:1863–1871

47. Goldberg L, Kloog Y (2006) A Ras inhibitor tilts the balance between Rac and Rho and blocks phosphatidylinositol 3-kinase-dependent glioblastoma cell migration. Cancer Res 66:11709–11717
48. Welch HCE, Coadwell WJ, Stephens LR, Hawkins PT (2003) Phosphoinositide 3-kinase-dependent activation of Rac. FEBS Lett 546:93–97
49. Han J, Luby-Phelps K, Das B, Shu X, Xia Y, Mosteller RD, Krishna UM, Falck JR, White MA, Broek D (1998) Role of substrates and products of PI 3-kinase in regulating activation of Rac-related guanosine triphosphatases by Vav. Science 279:558–560
50. Konno D, Yoshimura S, Hori K (2005) Involvement of the phosphatidylinositol 3-kinase/Rac1 and Cdc42 pathways in radial migration of cortical neurons. J Biol Cell 280:5082–5088
51. Kitagawa M, Aonuma M, Lee SH, Fukutake S, Fukytake S, McCormick F (2008) E2F-1 transcriptional activity is a critical determinant of Mdm2 antagonist-induced apoptosis in human tumor cell lines. Oncogene 27:5303–5314
52. Ambrosini G, Sambol EB, Carvajal D, Vassilev LT, Singer S, Schwartz GK (2006) Mouse double minute antagonist Nutlin-3a enhances chemotherapy-induced apoptosis in cancer cells with mutant p53 by activating E2F1. Oncogene 26:3473–3481